Biochemical Systematics and Ecology 61 (2015) 493–500

Contents lists available at ScienceDirect

Biochemical Systematics and Ecology

journal homepage: www.elsevier.com/locate/biochemsyseco

Mitochondrial phylogeography of a surf clam *Mactra veneriformis* in the East China Sea: Genetic homogeneity across two biogeographic boundaries

Gang Ni, Qi Li*, Lingfeng Kong, Hong Yu

The Key Laboratory of Mariculture, Ministry of Education, Ocean University of China, Qingdao, China

ARTICLE INFO

Article history:
Received 16 March 2015
Received in revised form 13 July 2015
Accepted 17 July 2015
Available online xxx

Keywords:
Population structure
Intertidal invertebrates
Glacial refugium
Geographic barrier
Marginal sea

ABSTRACT

Biogeographic boundaries constraining species' distributions often generate intraspecific 'breaks' for those species whose ranges span them—known as the 'biogeography-phylogeography concordance' hypothesis. The East China Sea (ECS) in the northwestern Pacific comprises two reported boundaries: the Shandong Peninsula and the Changjiang Estuary, providing an elegant setting to test the hypothesis in marine environment. Here we investigated population structure of the surf clam *Mactra veneriformis* (Reeve, 1854) using 235 individuals from its major distribution in the ECS, represented by mitochondrial cytochrome oxidase I sequences. A 'star-like' topology with shallow divergence was revealed for all haplotypes, of which the central (also assumed ancestral) one appearing in all populations. No significant genetic structure was revealed among populations, suggesting substantial genetic homogeneity across the range. Demographic expansion was revealed for individual and overall populations, and the expansion time was estimated from 23,000 years ago. These results suggested that the *M. veneriformis* populations originated from an ancestral panmictic population in the ECS basin, and had experienced significant population expansion since the last glacial maximum. From a mitochondrial view, the two boundaries did not act as barriers for the phylogeography of *M. veneriformis*.

1. Introduction

The biogeography and phylogeography concordance hypothesis indicates that biogeographic province boundaries constraining species' spatial ranges often generate intraspecific genetic structure for those species whose ranges span them (Brante et al., 2012). In marine realms, explicit boundaries often lie where nearshore ocean currents with sharply differing characteristics collide, forming striking physical and ecological gradients that potentially limit species' distribution ranges and intraspecific gene flow (McCartney et al., 2013). Well-known examples are from the coastline of North and South America, including Cape Hatteras (McCartney et al., 2013), the Point Conception (Eberl et al., 2013) and the Amazon–Orinoco outflow (Rocha et al., 2002). However, for the vast region of the northwestern (NW) Pacific, few studies have been conducted to shed light on the hypothesis, and little is known about genetic response of intertidal species to physical boundaries in the region.

* Corresponding author.
E-mail address: qili66@ouc.edu.cn (Q. Li).

http://dx.doi.org/10.1016/j.bse.2015.07.026
0305-1978/

The East China Sea (ECS) with the Bohai (BH) and Yellow Sea (YS) spans latitude 41°N to 23°N in the NW Pacific (Fig. 1). It comprises two reported biogeographic boundaries: the Shandong (SD) Peninsula and the Changjiang (CJ) Estuary, providing an ideal setting to test the concordance hypothesis in marginal seas. The SD Peninsula, situated in the eastern part of Shandong Province, is the largest peninsula in China. The Chengshan (CS) Cape in the easternmost of the peninsula is a boundary to divide the YS into north and south parts along coastal China (Liu, 2013). However it is not a barrier for coastal currents across the YS, as the Lubei Coastal Current, issuing from the BH and flowing along the north coast of SD Peninsula, can turn south and westward from the CS Cape into the south YS (Fig. 1). Recent genetic studies suggested the peninsula was responsible for species assemblages of some intertidal species, such as the genus *Ligia* (Yin et al., 2013). On the intraspecific level, populations in the BH and south YS were found to have evolved independently because of the isolation of the peninsula (*e.g.* bivalve, Ni et al., 2011; clam worm, Qin et al., 2013), sometimes even for fish with a relatively long dispersal ability (*e.g.* *Pampus argenteus*, Qin et al., 2013).

Another boundary lies in the CJ Estuary (31° N). As the third largest river in the world, the Changjiang River enters the ECS with huge freshwater outflow named Changjiang Diluted Water (CDW), which collides with the southward Subei Coastal Current and the northward China Coastal Current (Su and Yuan, 2005) (Fig. 1). Marked changes in coastal topology, salinity, temperature, nutrient conditions and planktonic community occur in the vicinity of the estuary (Wang et al., 2003; Su and Yuan, 2005; Chen et al., 2009). These factors may act in combination on biota's distribution. In fact, the estuary has been long proposed as biogeographic boundary separating two Chinese molluscan faunal regions: I Far East Subregion of North Pacific Region; II Sino-Japanese Subregion of Indo-West Pacific Region (Zhang et al., 1963). I represents a warm temperate region inhabited by northern warm-water species, and II is a subtropical region harboring rich subtropical molluscan fauna. However, whether the estuary serves as a phylogeographic barrier for molluscs is still controversial. Xu (1997) pointed out the boundary was not insurmountable for some wide-distributed species, and evidence from bivalves *Cyclina sinensis* (Ni et al., 2012) and *Atrina pectinata* (Liu et al., 2011b) supports the view. While for other species, a barrier effect was revealed, *e.g.* gastropod *Cellana toreuma* (Dong et al., 2012) and bivalve *Coelomactra antiquata* (Kong et al., 2007).

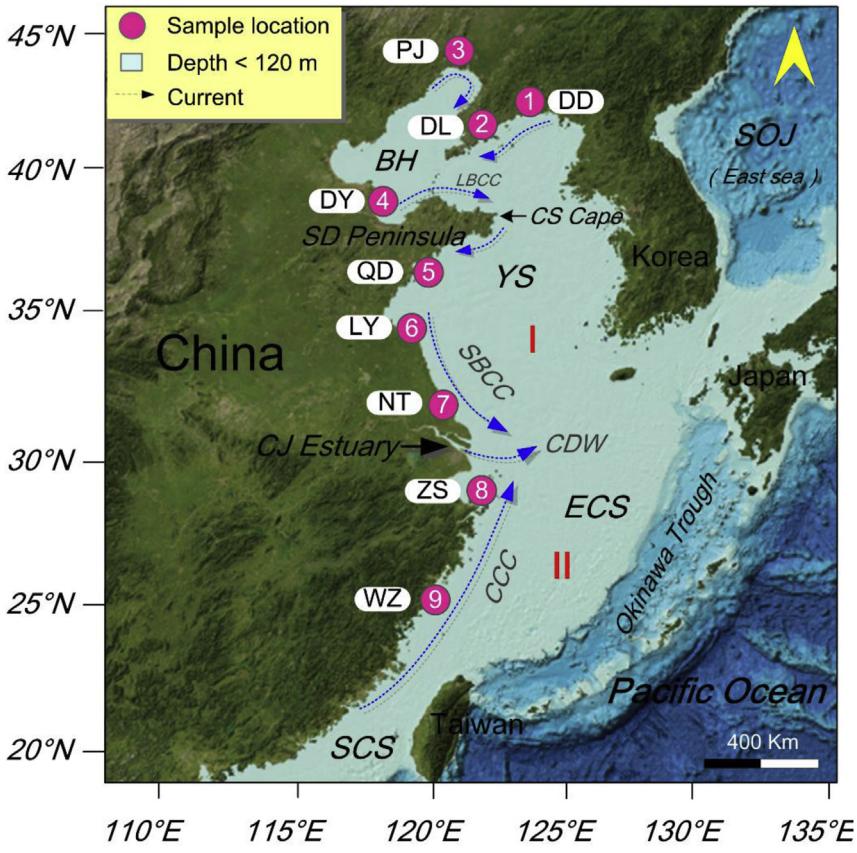

Fig. 1. Map of the northwestern Pacific showing the sampling sites of *Mactra veneriformis*. Populations are labeled with abbreviations and numbers as shown in Table 1. *LBCC*: Lubei Coastal Current; *SBCC*: Subei Coastal Current; *CDW*: Changjiang Diluted Water; *CCC*: China Coastal Current; SD: Shandong; CJ: Changjiang; CS: Chengshan; BH: Bohai; YS: Yellow Sea; ECS: East China Sea; SCS: South China Sea; SOJ: Sea of Japan. I: Far East Subregion of North Pacific Region; II: Sino-Japanese Subregion of Indo-West Pacific Region (Zhang et al., 1963). The seafloor topographic map is modified from General Bathymetric Chart of the Oceans (GEBCO: www.gebco.net/).

In this study, we aim to test the intraspecific barrier effect of the two boundaries on an intertidal species—the surf clam *Mactra veneriformis* (Mollusca, Bivalvia, Mactridae). The species is a temperate bivalve with distribution in China, Korea and Japan, usually found burrowed in sand or muddy sand bottom from low-tide level to shallow waters (Qi, 2004). Although little is known about how far adult *M. veneriformis* can travel, the species is characterized by high fecundity ($>10^6$ eggs per female) and a pelagic larval duration (PLD) up to 10 days (Wang and Wang, 2008), which may potentially facilitate gene flow via coastal currents. On the other hand, coastal invertebrates was essentially one-dimensional, occupying a narrow strip of shoreline range (Sagarin and Gaines, 2002). In contrary to open-sea species, their population structure is prone to be shaped by barriers from biogeographic, physical and historical factors (Kelly and Palumbi, 2010). Here we will reveal the population structure of *M. veneriformis* in the ECS using sequences from a fragment of the mitochondrial cytochrome oxidase I (COI), and test if there are intraspecific breaks corresponding to the known biogeographic boundaries from a mitochondrial view.

2. Materials and methods

2.1. Sample collection

Specimens of *M. veneriformis* were obtained from nine locations along its major distribution range in the ECS. As this species is a common bivalve, no specific permit is required for collection. Efforts were made to reach a relatively intense sampling for each site. Finally, a total of 235 individuals were collected from May 2006 and August 2009, with 22–32 specimens for each population. The adductor muscle was incised from samples and stored in 100% ethanol immediately. Total genomic DNA was extracted from muscle tissue using a standard phenol-chloroform purification procedure as described by Li et al. (2002).

2.2. DNA extraction, PCR and sequencing

We amplified a fragment of COI gene for each specimen using the universal primers LCO-1490 (5′-GGTCAACAAATCA-TATTG-3′) and HCO-2198 (5′- TAAACTTCAGGGTGACCAAAAAATCA-3′) (Folmer et al., 1994). Each polymerase chain reaction (PCR) was carried out in 50-μL volumes including 2 U *Taq* DNA polymerase (Takara), about 100 ng of total genomic DNA, 0.25 μM of each primer, 0.2 mM dNTP mix, 2 mM $MgCl_2$ and 5 μL 10 × PCR buffer. PCR was performed on a GeneAmp® 9700 PCR System (Applied Biosystems) following the cycling parameters in Ni et al. (2012). The PCR products were confirmed by 1.5% TBE agarose gel electrophoresis stained with ethidium bromide, and then cleaned using the EZ Spin Column PCR Product Purification Kit (Sangon) following described protocol. The cleaned product was prepared for sequencing using the BigDye Terminator Cycle Sequence Kit (ver. 3.1, Applied Biosystems) and finally sequenced on an ABI PRISM 3730 automatic sequencer.

2.3. Sequence variation and population structure analyses

Sequences were edited and aligned using the DNAstar software suite (DNASTAR, Madison, Wis.) with a final recheck by eye. Haplotypes were defined using the DnaSP 5 (Librado and Rozas, 2009) and deposited in GenBank database with accession numbers KC205728–KC205861. Their topology were inferred by a network analysis constructed in the TCS 1.21 (Clement et al., 2000), which was suitable to visualize close intraspecific relationships. The best-fit evolutionary model was selected using the jModelTest 2 (Darriba et al., 2012) under the Akaike information criterion. Finally GTR + I model was chosen and used in subsequent analyses.

The software ARLEQUIN 3.5 (Excoffier and Lischer, 2010) was used to calculate molecular diversity indices such as polymorphic sites, haplotype (h) and nucleotide diversity (π). The nucleotide sequences were translated to protein sequences using MEGA 6 (Tamura et al., 2013) and variable sites were calculated. A spatial analysis of molecular variance (SAMOVA) (Dupanloup et al., 2002) was conducted to define groups of populations as geographically homogeneous with tested K ranging from 2 to 8. The partitioning of genetic variation was then estimated using a hierarchical analysis of molecular variance (AMOVA, Excoffier et al., 1992) in ARLEQUIN with 10,000 permutations. As the GTR + I model was not available in ARLEQUIN, the closest one—Tamura and Nei (1993) model was applied. Pairwise Φ_{ST} was also calculated under this model with 1000 random replicates in ARLEQUIN followed by a standard Bonferroni correction (Rice, 1989). The association between the genetic similarity $[F_{ST}/(1-F_{ST})]$ (Slatkin, 1995) and geographical distances (log-transformed) was examined with Mantel tests in IBD web service (Jensen et al., 2005), using permutation methods (10,000 randomizations).

2.4. Historical demography

Demographic expansion was evaluated for each population using Tajima' D (Tajima, 1989) and Fu's F_S neutrality tests (Fu, 1997) as implemented in ARLEQUIN with 10,000 bootstrap replicates. For populations showing signals of expansion, mismatch distribution was performed to test whether they underwent a sudden expansion model. The sum-of-squared-differences (SSD) statistic (Harpending, 1994) was used to test the goodness-of-fit between the observed and expected mismatch distributions (10,000 replicates). As no divergent lineages was revealed (see Results), we also conducted neutral tests and mismatch distribution for the overall populations. The expansion parameter (τ) was estimated and transformed to

the real time since expansion. As far as we know, there is neither an accurate mutation rate nor a clear fossil record available for the species. Mutation rates used in former molluscan studies, ranging from 0.35 to 1.2% per million years (myr^{-1}), were usually estimated from deep splits of interspecific phylogeny (*e.g.* Hellberg and Vacquier, 1999; Marko, 2002; Lessios, 2008; Liu et al., 2011b). This approach however was recently questioned because more evidence showed that transient mutations accumulated in populations more quickly than that fixed in phylogenetic divergences, known as the 'time-dependent mutation rate' hypothesis (Ho et al., 2005). Evidence from previous studies indicated that mutation rate under the hypothesis might be an order of magnitude faster than that based on a phylogenetic calibration (Ho et al., 2008; Grant et al., 2012). So we applied here a tenfold faster mutation rate 10% myr^{-1} than that used in former studies (1% myr^{-1}, Marko et al., 2010) to shed light on a recent demographic scenario (also see Liu et al., 2011a).

Historical demography was also inferred using Bayesian skyline plot (BSP, Drummond et al., 2005) implemented in BEAST 1.81 (Drummond and Rambaut, 2007). A mutation rate of 10% myr^{-1} and a generation time of one year (Wang and Wang, 2008) were assigned to convert the parameter to real expansion time. Analyses were run for 100 million generations and sampled every 1000 steps with the first 10 million generations discarded as burn-in. We repeated the analyses using different random number seeds to check the reliability. The effective population size values for the parameters were ensued over 300 in all runs. Tracer 1.6 was used to check and visualize the results (available from http://beast.bio.ed.ac.uk/Tracer).

3. Results

3.1. Sequence variation

A 627-bp alignment of the 235 nucleotide sequences revealed 110 polymorphic sites with 99 transitions, 18 transversions and no indels, defining a total of 134 haplotypes. When translated to protein sequences, nine variable sites including two parsimony-informative sites were suggested. The number of haplotypes per population ranged from 17 in DY to 24 in ZS, and the haplotype diversity was observed overall high with the lowest $h = 0.942$ in two populations. The estimated nucleotide diversity ranged from 0.00447 in DL to 0.00848 in QD (Table 1). The parsimony network of the haplotypes showed a 'star-like' topology with shallow genetic divergence (Fig. 2). The central haplotype H.1 was found in all populations with a dominate number of 41 copies (17.4%). No more than seven mutation steps were required to connect it with the peripheral haplotypes. Some internal ones such as H.2–4 were also abundant and distributed in at least four populations, without clear spatial patterns.

3.2. Population structure analyses

The SAMOVA analyses identified the optimal grouping option for which the F_{CT} was highest. Here the highest value appeared at two groups [(DD, DL, PJ, DY, LY, NT, ZS, WZ); (QD)]. The AMOVA analysis based on the grouping, however, indicated a non-significant level of genetic structure among groups ($\Phi_{CT} = 0.0261$, $P = 0.1095$). The majority of genetic variation (97.44%) was attributed to variation within populations ($\Phi_{ST} = 0.0256$), with little explained by variation among populations within groups ($\Phi_{SC} = -0.0005$). For pairwise Φ_{ST}, although three comparisons were calculated with $P > 0.05$, but they were not significant after Bonferroni corrections (Table 2). The genetic and geographic distance matrices of *M. veneriformis* were not significantly associated in the IBD analysis ($r = 0.105$, $P = 0.275$).

3.3. Historical demography

Except the D value of QD, Tajima' D and Fu' F_S tests yielded significantly negative values for all populations, indicating each one had experienced a demographical expansion under the neutral model (all $P < 0.05$; Table 3). The subsequent goodness-of-fit tests supported the null hypothesis of a sudden expansion model with nonsignificant values for SSD (all $P > 0.05$). When

Table 1
Sample information and diversity indices for each population of *Mactra veneriformis*.

Sample site (Abbr.)	Lat. (°N)/Lon. (°E)	*N*	*n*	*h*	π
1. Dandong (DD)	39.82/124.27	25	19	0.970 (0.022)	0.00721 (0.00409)
2. Dalian (DL)	38.87/121.63	28	18	0.942 (0.030)	0.00447 (0.00271)
3. Panjin (PJ)	40.71/121.80	27	20	0.954 (0.028)	0.00653 (0.00374)
4. Dongying (DY)	37.48/118.96	25	17	0.950 (0.027)	0.00615 (0.00356)
5. Qingdao (QD)	36.03/120.37	22	20	0.991 (0.017)	0.00848 (0.00475)
6. Lianyungang (LY)	34.69/119.50	28	21	0.955 (0.030)	0.00596 (0.00345)
7. Nantong (NT)	31.94/121.87	23	19	0.984 (0.017)	0.00632 (0.00366)
8. Zhoushan (ZS)	30.03/122.25	32	24	0.942 (0.035)	0.00533 (0.00312)
9. Wenzhou (WZ)	27.89/120.90	25	19	0.947 (0.037)	0.00606 (0.00352)
Total		235	134		

N: number of individuals; *n*: number of haplotypes; *h*: haplotype diversity (with standard deviation); π: nuclear diversity (with standard deviation). Abbr., site abbreviation, Lat., latitude, Lon., longitude.

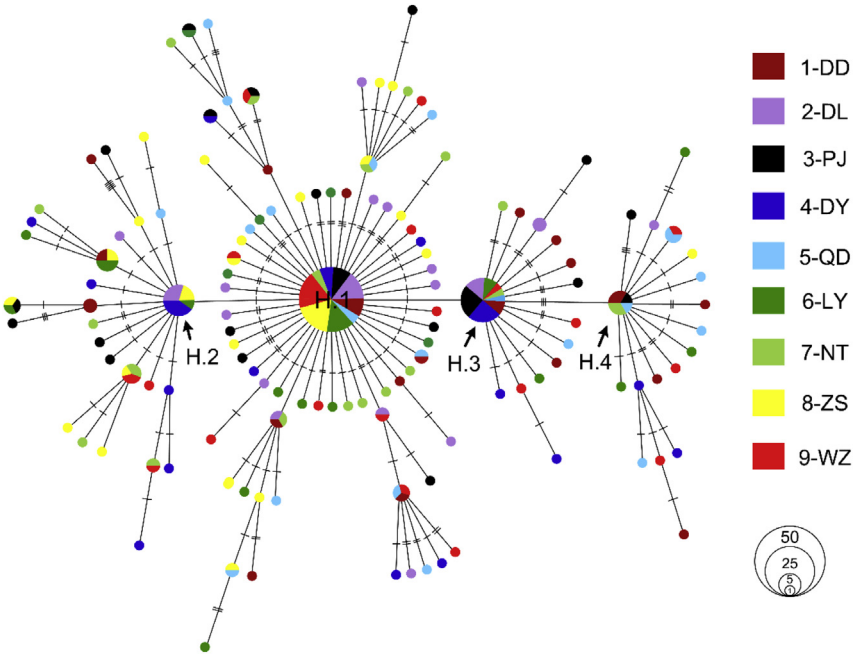

Fig. 2. Parsimony haplotype network for *Mactra veneriformis*. Each circle represents a single haplotype sized in proportion to its frequency. Bars indicate mutation steps between haplotypes.

the populations were treated as a whole, neutral tests were also calculated significantly negative ($D = -2.42$, $P < 0.05$; $F_S = -25.63$, $P < 0.05$). The mismatch analysis revealed a unimodal frequency distribution with $\tau = 2.88$ (95% confidence level: 1.38–6.15). The real expansion time was calculated from 23,000 (11,000–49,000) years ago, approximately corresponding to the last glacial maximum (LGM: 19,000–22,000 years ago; Yokoyama et al., 2000). The result was supported by reconstruction of effective population size through time in BSP: the population size of *M. veneriformis* experienced an expansion throughout the entire demographic history happened about 30,000 years ago (figure not shown), with a significant increase from about 18,000 years ago, after the LGM.

4. Discussion

Complex interactions exist between biological evolution and topographic features (Beheregaray, 2008). Recent phylogeographic studies revealed intraspecific splits often occur at biogeographic boundaries, suggesting general causative factors (McCartney et al., 2013). In marine realms, ideal geographic settings to test the 'biogeography-phylogeography concordance' hypothesis are not generally available, because environmental gradients in the ocean are neither as steep nor as immutable as on land (*e.g.* mountains and deserts) (Gaylord and Gaines, 2000). The ECS, characterized by unique tectonic and hydrological settings, provides a chance for us to understand genetic response of intertidal species to biogeographic boundaries in peripheral ecosystems.

4.1. Origin and demography of *M. veneriformis* populations

In this study, a 'star-like' topology with shallow genetic divergence was revealed for all haplotypes without clear geographic patterns. The central haplotype H.1, also being assumed the ancestral one based on Posada and Crandall (2001), appeared in all populations. This pattern indicated the origin of current *M. veneriformis* populations from a common ancestral population, which probably had survived in the ECS refugium.

The ECS was featured by a shallow and extensive continental shelf with a total area of 850,000 km^2. When the sea level declined about 130–150 m during the glacial periods, the shelf was completely exposed to land (Xie et al., 1995). The sea retreated to an elongate and curved basin—the Okinawa Trough with an area of its 1/3 present size (Wang, 1999). Marine species, especially coastal invertebrates experiencing a direct loss of habitat, were forced to migrate into the basin (Liu et al., 2007; Ni et al., 2012). Different populations got chances to mix together and formed a panmictic population there (Liu et al., 2011b). After the LGM, the survived biota might migrate out and quickly repopulate along the coastline following the flooding (Liu et al., 2007). These populations were expected to carry similar genetic signals as they were derived from an ancestral population. Expect *M. veneriformis*, the pattern was also observed for other co-distributed species in a meta-analysis of

Table 2
Pairwise Φ_{ST} among *Mactra veneriformis* populations.

Sites	DD	DL	PJ	DY	QD	LY	NT	ZS	WZ
DD	–								
DL	0.175	–							
PJ	−0.002	−0.003	–						
DY	−0.006	0.006	−0.005	–					
QD	−0.009	0.037*	0.012	0.020	–				
LY	−0.004	0.000	−0.011	0.001	0.011	–			
NT	0.005	0.007	−0.015	−0.009	0.009	−0.013	–		
ZS	0.035*	0.015	0.015	0.016	0.052*	0.001	−0.006	–	
WZ	0.001	−0.015	−0.012	−0.005	0.006	−0.004	−0.012	0.007	–

*$P < 0.05$ after 10,000 permutations but not significant after Bonferroni corrections.

Table 3
Estimates of neutral tests (Tajima' *D* and Fu' F_S) for each population and the mismatch distribution parameter SSD.

Population	Tajima' *D*		Fu' F_S		Goodness-of-fit test	
	D	*P*	F_S	*P*	SSD	*P*
1. DD	−1.7314	0.0257	−12.2109	0.0000	0.0011	0.9180
2. DL	−2.2098	0.0033	−13.3961	0.0000	0.0027	0.4610
3. PJ	−2.1159	0.0052	−13.9193	0.0000	0.0062	0.4420
4. DY	−1.8149	0.0178	−9.8661	0.0000	0.0017	0.8390
5. QD	−1.1430	0.1228	−15.7503	0.0000	0.0033	0.6110
6. LY	−2.0224	0.0060	−16.5973	0.0000	0.0009	0.8910
7. NT	−1.5646	0.0414	−15.0964	0.0000	0.0080	0.2180
8. ZS	−2.0926	0.0050	−22.6393	0.0000	0.0002	0.9920
9. WZ	−1.9046	0.0139	−13.9882	0.0000	0.0023	0.7720

different ECS taxonomic groups (including fishes, molluscs and crustaceans), collectively supporting the ECS origin hypothesis (Ni et al., 2014).

Demographic expansion was inferred for individual and overall populations based on multiple evidences from neutral tests, mismatch distribution and BSP. For the whole species, the real time since expansion was calculated from about 23,000 to 18,000 years ago in mismatch distribution and BSP analyses, respectively, roughly corresponding to the LGM. Globally, this period was reported the most important period affecting population demography (Hewitt, 2004). Previous climate cycles could also have effects on population fluctuations, but the signals might have been erased by population declines during the LGM (Grant et al., 2012). Note, the time frame in this study was calculated under the 'time-dependent mutation rate' hypothesis. As this hypothesis is still controversial (*e.g.* Bandelt, 2007) and the mutation rate applied was chosen based on experience of former studies, demographic conclusions abstracted here should be treated with caution. Lack of fossil record and ancestral DNA represents a major hurdle for accurate mutation rate estimation of marine invertebrates (Provan and Bennett, 2008). Further evidence from the radiocarbon ages of ancient samples or biogeography can provide internal calibrations for a specific species (Ho et al., 2008), which may greatly benefit the demography estimation of marine species.

4.2. Genetic homogeneity and possible explanations

Despite the SD Peninsula and CJ Estuary were reported to be responsible for both species assemblages and intraspecific splits in several studies (*e.g.* Zhang et al., 1963; Ni et al., 2011; Dong et al., 2012), no barrier effect was indicated for the clam *M. veneriformis* based on mitochondrial DNA. Nonsignificant population structure was suggested in multiple analyses including the AMOVA, pairwise population comparisons and IBD analysis. The AMOVA analysis indicated that most genetic variation was attributed to differentiation within populations (97.44%), with variation among groups only explaining 2.61% of the total variation, indicating substantial genetic homogenous among populations. No genetic differentiation exhibited between pairwise comparisons of populations after Bonferroni corrections, and the IBD model was rejected in a Mantel analysis ($P = 0.275$). These results were supported by a former study based on nuclear genes (28S rRNA and ITS1), as high gene flow was indicated among the ECS populations and little differentiation was revealed (Zhang, 2008). However in another study applying Inter-Simple Sequence Repeats, substantial population subdivision was revealed and an IBD pattern was suggested to be responsible for the differentiation (Hou et al., 2006). This disconcordance suggested the importance of applying multiple markers with different resolution to understand species' phylogeographic patterns.

Several mechanisms were suspected to be responsible for the mitochondrial homogenous of *M. veneriformis* in this study. First these populations were expected to origin from a single panmictic population as discussed above, and there might lack sufficient time for complete lineage sorting after the recolonization in about 20,000 years. The same pattern was also observed in other co-distributed species, including fish (Zhang et al., 2014), shrimp (Li et al., 2009) and mollusc (Yang et al., 2008). Second, the spawning of the clam lasts from July to September (Ke and Li, 2013); coupled with a PLD of 10 days, these

life-history characteristics may facilitate the gene flow among populations via currents. The influence of ocean currents on contemporary gene flow had also been revealed by studies on fish and barnacle (Cheang et al., 2012; Han et al., 2012). Third, this species is abundant and with a continuous distribution along the ECS coastline (Qi, 2004); high genetic variation were measured in all sampling sites, indicating a large effective population size (Frankham, 1996). Such populations were insensitive to the loss and reorganization of variation by genetic drift, and could maintain the ancestral genetic information (Ellstrand and Elam, 1993). Additionally, as a commercially important species, juvenile clams of *M. veneriformis* were often translocated among sites for aquaculture purpose (Hou et al., 2006). Human-aided dispersal may enhance gene flow between source and introduced populations, causing the mixture of gene pool. Similar cases have been revealed for pearl oyster *Pinctada margaritifera cumingii* (Arnaud-Haond et al., 2004) and blood clam *Tegillarca granosa* (Ni et al., 2012).

Acknowledgments

We are indebted to Dr Jun Chen from Linyi University and Dr Hongtao Nie from Dalian Ocean University for their kind assistance in specimen collection. This study was supported by research grants from National Natural Science Foundation of China (41276138), National Marine Public Welfare Research Program (201305005), and Doctoral Program of Ministry of Education of China (20130132110009).

References

Arnaud-Haond, S., Vonau, V., Bonhomme, F., Boudry, P., Blanc, F., Prou, J., Seaman, T., Goyard, E., 2004. Spatio-temporal variation in the genetic composition of wild populations of pearl oyster (*Pinctada margaritifera cumingii*) in French Polynesia following 10 years of juvenile translocation. Mol. Ecol. 13, 2001–2007.
Bandelt, H.-J., 2007. Time dependency of molecular rate estimates: tempest in a teacup. Heredity 100, 1–2.
Beheregaray, L.B., 2008. Twenty years of phylogeography: the state of the field and the challenges for the Southern Hemisphere. Mol. Ecol. 17, 3754–3774.
Brante, A., Fernández, M., Viard, F., 2012. Phylogeography and biogeography concordance in the marine gastropod *Crepipatella dilatata* (Calyptraeidae) along the southeastern Pacific coast. J. Hered. 103, 630–637.
Cheang, C.C., Tsang, L.M., Ng, W.C., Williams, G.A., Chu, K.H., Chan, B.K., 2012. Phylogeography of the cold-water barnacle *Chthamalus challengeri* in the north-western Pacific: effect of past population expansion and contemporary gene flow. J. Biogeogr. 39, 1819–1835.
Chen, C.C., Shiah, F.K., Chiang, K.P., Gong, G.C., Kemp, W.M., 2009. Effects of the Changjiang (Yangtze) River discharge on planktonic community respiration in the East China Sea. J. Geophys. Res. 114, C03005.
Clement, M., Posada, D., Crandall, K.A., 2000. TCS: a computer program to estimate gene genealogies. Mol. Ecol. 9, 1657–1659.
Darriba, D., Taboada, G.L., Doallo, R., Posada, D., 2012. jModelTest 2: more models, new heuristics and parallel computing. Nat. Methods 9, 772–772.
Dong, Y.W., Wang, H.S., Han, G.D., Ke, C.H., Zhan, X., Nakano, T., Williams, G.A., 2012. The impact of Yangtze river discharge, ocean currents and historical events on the biogeographic pattern of *Cellana toreuma* along the China coast. PLoS One 7, e36178.
Drummond, A.J., Rambaut, A., 2007. BEAST: Bayesian evolutionary analysis by sampling trees. BMC Evol. Biol. 7, 214.
Drummond, A.J., Rambaut, A., Shapiro, B., Pybus, O.G., 2005. Bayesian coalescent inference of past population dynamics from molecular sequences. Mol. Biol. Evol. 22, 1185–1192.
Dupanloup, I., Schneider, S., Excoffier, L., 2002. A simulated annealing approach to define the genetic structure of populations. Mol. Ecol. 11, 2571–2581.
Eberl, R., Mateos, M., Grosberg, R.K., Santamaria, C.A., Hurtado, L.A., 2013. Phylogeography of the supralittoral isopod *Ligia occidentalis* around the Point Conception marine biogeographical boundary. J. Biogeogr. 40, 2361–2372.
Ellstrand, N.C., Elam, D.R., 1993. Population genetic consequences of small population size: implications for plant conservation. Annu. Rev. Ecol. Syst. 24, 217–242.
Excoffier, L., Lischer, H.E.L., 2010. Arlequin suite ver 3.5: a new series of programs to perform population genetics analyses under Linux and Windows. Mol. Ecol. Resour. 10, 564–567.
Excoffier, L., Smouse, P.E., Quattro, J.M., 1992. Analysis of molecular variance inferred from metric distances among DNA haplotypes: application to human mitochondrial DNA restriction data. Genetics 131, 479–491.
Folmer, O., Black, M., Hoeh, W., Lutz, R., Vrijenhoek, R., 1994. DNA primers for amplification of mitochondrial cytochrome c oxidase subunit I from diverse metazoan invertebrates. Mol. Mar. Biol. Biotechnol. 3, 294–299.
Frankham, R., 1996. Relationship of genetic variation to population size in wildlife. Conserv. Biol. 10, 1500–1508.
Fu, Y.X., 1997. Statistical tests of neutrality of mutations against population growth, hitchhiking and background selection. Genetics 147, 915–925.
Gaylord, B., Gaines, S.D., 2000. Temperature or transport? Range limits in marine species mediated solely by flow. Am. Nat. 155, 769–789.
Grant, W.S., Liu, M., Gao, T., Yanagimoto, T., 2012. Limits of Bayesian skyline plot analysis of mtDNA sequences to infer historical demographies in Pacific herring (and other species). Mol. Phylogen. Evol. 65, 203–212.
Harpending, H., 1994. Signature of ancient population growth in a low-resolution mitochondrial DNA mismatch distribution. Hum. Biol. 66, 591–600.
Han, Z.Q., Yanagimoto, T., Zhang, Y.P., Gao, T.X., 2012. Phylogeography study of *Ammodytes personatus* in northwestern Pacific: Pleistocene isolation, temperature and current conducted secondary contact. PLoS One 7, e37425.
Hellberg, M.E., Vacquier, V.D., 1999. Rapid evolution of fertilization selectivity and lysin cDNA sequences in teguline gastropods. Mol. Biol. Evol. 16, 839–848.
Hewitt, G., 2004. Genetic consequences of climatic oscillations in the Quaternary. Philos. Trans. R. Soc. B Biol. Sci. 359, 183–195.
Ho, S.Y.W., Phillips, M.J., Cooper, A., Drummond, A.J., 2005. Time dependency of molecular rate estimates and systematic overestimation of recent divergence times. Mol. Biol. Evol. 22, 1561–1568.
Ho, S.Y.W., Saarma, U., Barnett, R., Haile, J., Shapiro, B., 2008. The effect of inappropriate calibration: three case studies in molecular ecology. PLoS One 3, e1615.
Hou, L., Lü, H., Zou, X., Bi, X., Yan, D., He, C., 2006. Genetic characterizations of *Mactra veneriformis* (Bivalve) along the Chinese coast using ISSR-PCR markers. Aquaculture 261, 865–871.
Jensen, J., Bohonak, A., Kelley, S., 2005. Isolation by distance, web service. BMC Genet. 6, 13.
Ke, Q.Z., Li, Q., 2013. Annual dynamics of glycogen, lipids, and proteins during the reproductive cycle of the surf clam *Mactra veneriformis* from the north coast of Shandong Peninsular, China. Invertebr. Reprod. Dev. 57, 49–60.
Kelly, R.P., Palumbi, S.R., 2010. Genetic structure among 50 species of the northeastern Pacific rocky intertidal community. PLoS One 5, e8594.
Kong, L.F., Li, Q., Qiu, Z.X., 2007. Genetic and morphological differentiation in the clam *Coelomactra antiquata* (Bivalvia: Veneroida) along the coast of China. J. Exp. Mar. Biol. Ecol. 343, 110–117.
Lessios, H.A., 2008. The great American schism: divergence of marine organisms after the rise of the Central American Isthmus. Annu. Rev. Ecol. Evol. Syst. 39, 63–91.
Li, Q., Park, C., Kijima, A., 2002. Isolation and characterization of microsatellite loci in the Pacific abalone, *Haliotis discus hannai*. J. Shellfish Res. 21, 811–816.

Li, Y.L., Kong, X.Y., Yu, Z.N., Kong, J., Ma, S., Chen, L.M., 2009. Genetic diversity and historical demography of Chinese shrimp *Feneropenaeus chinensis* in Yellow Sea and Bohai Sea based on mitochondrial DNA analysis. Afr. J. Biotechnol. 8, 1193–1202.
Librado, P., Rozas, J., 2009. DnaSP v5: a software for comprehensive analysis of DNA polymorphism data. Bioinformatics 25, 1451–1452.
Liu, J.X., Tatarenkov, A., Beacham, T.D., Gorbachev, V., Wildes, S., Avise, J.C., 2011a. Effects of Pleistocene climatic fluctuations on the phylogeographic and demographic histories of Pacific herring (*Clupea pallasii*). Mol. Ecol. 20, 3879–3893.
Liu, J., 2013. Status of marine biodiversity of the China Seas. PloS One 8, e50719.
Liu, J., Li, Q., Kong, L.F., Zheng, X.D., 2011b. Cryptic diversity in the pen shell *Atrina pectinata* (Bivalvia: Pinnidae): high divergence and hybridization revealed by molecular and morphological data. Mol. Ecol. 20, 4332–4345.
Liu, J.X., Gao, T.X., Wu, S.F., Zhang, Y.P., 2007. Pleistocene isolation in the Northwestern Pacific marginal seas and limited dispersal in a marine fish, *Chelon haematocheilus* (Temminck and Schlegel, 1845). Mol. Ecol. 16, 275–288.
Marko, P.B., 2002. Fossil calibration of molecular clocks and the divergence times of geminate species pairs separated by the Isthmus of Panama. Mol. Biol. Evol. 19, 2005–2021.
Marko, P.B., Hoffman, J.M., Emme, S.A., Mcgovern, T.M., Keever, C.C., Nicole, C., 2010. The 'Expansion-Contraction' model of Pleistocene biogeography: rocky shores suffer a sea change? Mol. Ecol. 19, 146–169.
McCartney, M.A., Burton, M.L., Lima, T.G., 2013. Mitochondrial DNA differentiation between populations of black sea bass (*Centropristis striata*) across Cape Hatteras, North Carolina (USA). J. Biogeogr. 40, 1386–1398.
Ni, G., Li, Q., Kong, L.F., Yu, H., 2014. Comparative phylogeography in marginal seas of the northwestern. Pac. Mol. Ecol. 23, 534–548.
Ni, G., Li, Q., Kong, L.F., Zheng, X.D., 2012. Phylogeography of the bivalve *Tegillarca granosa* in coastal China: implications for management and conservation. Mar. Ecol. Prog. Ser. 452, 119–130.
Ni, L.H., Li, Q., Kong, L.F., 2011. Microsatellites reveal fine-scale genetic structure of the Chinese surf clam *Mactra chinensis* (Mollusca, Bivalvia, Mactridae) in Northern China. Mar. Ecol. 32, 488–497.
Posada, D., Crandall, K.A., 2001. Intraspecific gene genealogies: trees grafting into networks. Trends. Ecol. Evol. 16, 37–45.
Provan, J., Bennett, K.D., 2008. Phylogeographic insights into cryptic glacial refugia. Trends. Ecol. Evol. 23, 564–571.
Qi, Z.Y., 2004. Seashells of China. China Ocean Press, Beijing.
Qin, Y., Shi, G., Sun, Y., 2013. Evaluation of genetic diversity in *Pampus argenteus* using SSR markers. Gen. Mol. Res. 12, 5833.
Rice, W.R., 1989. Analyzing tables of statistical tests. Evolution 43, 223–225.
Rocha, L.A., Bass, A.L., Robertson, D.R., Bowen, B.W., 2002. Adult habitat preferences, larval dispersal, and the comparative phylogeography of three Atlantic surgeonfishes (Teleostei: Acanthuridae). Mol. Ecol. 11, 243–252.
Sagarin, R.D., Gaines, S.D., 2002. Geographical abundance distributions of coastal invertebrates: using one-dimensional ranges to test biogeographic hypotheses. J. Biogeogr. 29, 985–997.
Slatkin, M., 1995. A measure of population subdivision based on microsatellite allele frequencies. Genetics 139, 457.
Su, J.L., Yuan, Y.L., 2005. Coastal Hydrology of China. Ocean Press, Beijing (in Chinese).
Tajima, F., 1989. Statistical method for testing the neutral mutation hypothesis by DNA polymorphism. Genetics 123, 585.
Tamura, K., Nei, M., 1993. Estimation of the number of nucleotide substitutions in the control region of mitochondrial DNA in humans and chimpanzees. Mol. Biol. Evol. 10, 512–526.
Tamura, K., Stecher, G., Peterson, D., Filipski, A., Kumar, S., 2013. MEGA6: molecular evolutionary genetics analysis version 6.0. Mol. Biol. Evol. 30, 2725–2729.
Wang, B., Wang, X., Zhan, R., 2003. Nutrient conditions in the Yellow Sea and the East China sea. Estuar. Coast. Shelf Sci. 58, 127–136.
Wang, P.X., 1999. Response of western Pacific marginal seas to glacial cycles: paleoceanographic and sedimentological features. Mar. Geol. 156, 5–39.
Wang, R.C., Wang, Z.P., 2008. Science of Marine Shellfish Culture. China Ocean University Press, Qingdao (in Chinese).
Xie, C., Jian, Z., Zhao, Q., 1995. Paleogeographic Maps of the China Seas at the Last Glacial Maximum WESTPAC Paleogeographic Maps. UNESCO/IOC Publications, Shanghai.
Xu, F.S., 1997. Bivalve Mollusca of China Seas. Science Press, Beijing (in Chinese).
Yang, J.M., Li, Q., Zheng, X.D., Song, Z.L., Wang, R.C., 2008. Genetic diversity in populations of *Rapana venosa* in coastal waters of China. Oceanol. Limnol. Sin. 39, 257–262.
Yin, J., Pan, D., He, C., Wang, A., Yan, J., Sun, H., 2013. Morphological and molecular data confirm species assignment and dispersal of the genus *Ligia* (Crustacea: Isopoda: Ligiidae) along northeastern coastal China and East Asia. Zool. J. Linn. Soc. 169, 362–376.
Yokoyama, Y., Lambeck, K., de Deckker, P., Johnston, P., Fifield, I.K., 2000. Timing of the Last Glacial Maximum from observed sea-level minima. Nature 406, 713–716.
Zhang, H., Yanagimoto, T., Zhang, X., Song, N., Gao, T.X., 2014. Lack of population genetic differentiation of a marine ovoviviparous fish *Sebastes schlegelii* in Northwestern Pacific. Mitochondr. DNA 1–7.
Zhang, J., 2008. The Study of the Molecular Population Genetic and Phylogeny of *Mactra Veneriformis* Using 28SrRNA Gene and ITS1. Master's thesis. Liaoning Normal University (in Chinese with English abstract).
Zhang, X., Qi, Z.Y., Zhang, F.S., Ma, X.T., 1963. A preliminary study of the demarcation of marine molluscan faunal regions of and its adjacent waters. Oceanol. Limnol. Sin. 5, 124–138.